NN31545.0475

INSTITUUT VOOR CULTUURTECHNIEK EN WATERHUISHOUDING

NOTA 475, d.d. 29 juli 1968

Soil moisture measurement by the gamma transmission method

A. H. Ryhiner and J. Pankow

BIBLIOTHEEK
STARINGGEBOUW

Nota's van het Instituut zijn in principe interne communicatiemiddelen, dus geen officiële publikaties.
Hun inhoud varieert sterk en kan zowel betrekking hebben op een eenvoudige weergave van cijferreeksen, als op een concluderende discussie van onderzoeksresultaten. In de meeste gevallen zullen de conclusies echter van voorlopige aard zijn omdat het onderzoek nog niet is afgesloten.
Bepaalde nota's komen niet voor verspreiding buiten het Instituut in aanmerking.

1787739

1. Introduction

The development in atomic research has resulted in some modern methods for measuring soil moisture and soil density. The principal defects of the earlier methods used for this purpose, as soil sampling and the electrical resistance method with nylon units or gypsum blocks, are thereby overcome and in addition to a quicker measuring process, a remarkable increase in accuracy is obtained.

The present paper gives a discussion of the use of the gamma transmission method for the measurement of the variations in soil moisture in situ. Though the method is not specific for water, as is the case of the neutron scattering method, it has the advantage that the resolution thickness of the layer is much smaller. The neutron scattering technique is more suited to moisture content measurements of a large volume of soil, with a resolution over a distance of 15 cm in a wet to 30 cm in a dry soil.

Examples of work using the gamma transmission technique in laboratory studies of the water content in soil columns are given by GURR (1962) and DAVIDSON et al (1963). The high degree of resolution in these laboratory experiments is obtained by collimating the radiation beam at the source and at the detector, as well as by electronic discrimination against secondary, scattered radiation.

However, using this method for measurements on soil in situ the collimation at the source and at the detector is not practical and one has to use electronic discrimination only. REGINATO and VAN BAVEL (1964) showed, with an laboratory equipment, however, that it is critical to determine and to maintain the correct threshold value for the discriminator setting. Moreover, adjustments were necessary to compensate for electronic drift. Unpublished experiments performed by the present authors, using a battery fed field equipment, with a scintillation crystal combined with electronic discrimination, did show that it was practically impossible to reproduce the measured data after some time without large adjustments for electronic drift. The difficulties with the reproduction of the true values of the measured data, due to electronic drift, seems not to justify the use of an electronic discriminator setting in a field equipment. For this reason a series of experiments was performed with a field equipment in which no electronic discrimination of scattered radiation was applied.

2. Experimental procedure

2.1. Equipment

The equipment was constructed by Frieseke and Hoepfner, Erlangen-Bruck, Western Germany. The radiation source was a 20 mc Cs^{137} sealed source with a peak gamma energy of 0.662 Mev. The source was held in an access tube (o.d. 20 mm, i.d. 16 mm) by a for depth calibrated rod, which was connected by a frame to the brass rod which held the detector at the same depth as the source in its access tube (o.d. 40 mm, i.d. 36 mm). A scheme of the system is given in fig. 1. The detector was a proportional tube filled with halogen gas, connected with a preamplifier to an integrating counter system. The detector had a diameter of 32 mm and a height of 60 mm. The apparatus was fed by D.E.A.C. cells of 6 volt. The operational voltage was 650 volt. In the voltage range from 600 to 700 volt the count rate increased with 0.04% per volt.

An alignment jig was used to place the two access tubes parallel into the soil. Both positioning rods moved freely in the access tubes, so the possible deviations in the distance between the two access tubes were extremely small.

2.2. Calibration

Calibration was required to find the relation between count rate and density. For this purpose measurements were performed at a constant distance of 40 cm using concrete slabs with a known dry bulk density. The runs were made with dry slabs, as well as combined with water. The experiments were set up in such a way that the normal background effect was taken into account in the measurements. Copper, iron and plastic was used as material of the access tubes. The relation between count rate and density as obtained with the experiments with the dry slabs is presented in fig. 2. It appears that the relation between count rate and density strongly depends on the material used for the access tubes.

Fig. 3 shows the curves for the dry and the wet run in the iron access tubes. The dashed lines in this figure connect the points of equal dry bulk density in both runs. These lines represent approximately the relation between count rate and water content at a given value of the dry bulk density. It is clear from this figure that in fact for each value of the dry bulk density of the soil a new calibration curve has to be made which relates count rate with wet bulk density. This is also the case when one is interested in variations in soil moisture content alone, as the dashed lines are not parallel.

2. [illegible]

2.1. [illegible]

A third experiment was performed in water, so with a constant density, in which the distance between source and counter was varied. The results of this experiment are presented in fig. 4, in which count rate times the square of the distance is plotted against the distance. The strong deviation from linearity at short distance is caused by the instrumental resolution time, which is for this type of detectors in the order of 100 to 200 μ sec.

3. Discussion

With an excellent discrimination of all gamma energies below the primary emission, the radiation intensity will follow the inverse square-exponential law and the relation between radiation intensity and density is simple and predictable. In the presented experiments, however, no electronic discrimination has been applied, so the effect of scattered, secondary radiation must be taken into account. Moreover, when using halogen gas detectors, one must take into account the resolution time of the detector. The general expression for the relation between count rate and density can be given by the following equation:

$$\frac{I}{1 - I\tau} = \frac{I_o}{4\pi x^2} B\, e^{-\mu\rho x} \qquad (1)$$

where

$\frac{I_o}{4\pi}$ = unattenuated radiation intensity at a sphere of one cm radius;

I = actual radiation intensity;

x = length of the attenuation path;

μ = mass attenuation coefficient;

ρ = mass density;

B = build-up factor of scattered radiation;

τ = instrumental resolution time.

3.1. The mass attenuation coefficient

Strictly speaking, the 'electron density' and not the density of matter is determined, but with the various atoms (Si, O, Mg, Fe, Ca, Al), which give the composition of mineral soil, the ratio of the electron number (Z) to the mass number (A) is a half, with sufficient accuracy for elements having atomic numbers up to about Z = 26 (Fe). The only exception is hydrogen with a ratio equal to one. REGINATO and VAN BAVEL (1964) calculated the theoretical mass attenuation

A third exp[illegible] was performed in water, so with [illegible] instant density,
in which the distance [illegible] source and water was varied. The results [illegible] this
experiment are p[illegible] [illegible] ig. 4, in which [illegible] times the square of
distance is plotted [illegible] the ordinate. The resulting [illegible] ation from linearity at
distance is [illegible] the instrumental [illegible], which [illegible]
[illegible] ue of 100 mrad.

[illegible]cussion

[illegible] an exc[illegible] discrimination of all gamma [illegible] low the primary
emissi[illegible] [illegible] will follow the [illegible] ture upon initial
and the [illegible] intensity [illegible] impl[illegible]
in the presented [illegible] however, no [illegible] imination has be[illegible]
[illegible] secondary [illegible] be taken into
[illegible] thereby, [illegible] in coun[illegible]
[illegible] personal experience [illegible]
[illegible] the "flow p[illegible]

(1)

[illegible]

[illegible] in reading:

[illegible]

[illegible]

[illegible]

coefficients of nine representative oven-dry soils. The values differ only very slightly and the mean value of μ_s was 0.0775 $cm^2\ g^{-1}$. The theoretical mass attenuation coefficient of water is 0.0862 $cm^2\ g^{-1}$. The difference between the dry and the wet curve shown in fig. 3 must be explained by the different values of the mass attenuation coefficients. Soils which contain a large amount of organic matter even give a more deviating curve, as organic matter exists mainly of CH_2 - and OCH_3 groups. The weight ratio of both groups in organic matter is approximately equal to one.

The theoretical mass attenuation coefficients of the various soil constituents as well as the ratio ZA^{-1} are given in table 1. The ratio of the mass attenuation coefficients with respect to the one of water and the ratio of ZA^{-1} values with respect to water are also given.

Table 1. Mass attenuation coefficients and ZA^{-1} ratios of the various soil constituents

soil constituent	μ	ZA^{-1}	$\mu . \mu_w^{-1}$	$(ZA^{-1}) . (ZA^{-1})_w^{-1}$
mineral soil	0.0775	1/2	0.8991	0.9000
H_2O	0.0862	10/18	1.0000	1.0000
CH_2 - group	0.0883	8/14	1.0244	1.0286
OCH_3 - group	0.0848	17/31	0.9838	0.9871
organic matter	0.0866	243/434	1.0046	1.0078

Table 1 clearly demonstrates that the $\mu . \mu_w^{-1}$ ratio equals the $(ZA^{-1})\ (ZA^{-1})_w^{-1}$ ratio. This result practically means that when using the transmission method for moisture determinations one should not use at the horizontal axis of the calibration curve the sum of the mass densities of the various constituents but $0.9\ \rho_s + \rho_w + 1.01\ \rho_o$, where ρ_s is the dry bulk density of the mineral soil, ρ_w the volume fraction of water and ρ_o the bulk density of organic matter. In this case the densities of all soil constituents are expressed in the equivalent 'electron density' of water. In fig. 5 the data of the wet and dry run with the iron access tubes are presented with the equivalent density scale. The points of the dry and the wet run coincide perfectly. Using the proposed scale means that a single calibration curve is valid for very different soils.

3.2. The build-up factor and the resolution time

The deviation from linearity of the curves as presented in fig. 2 and fig. 4 is caused by the influence of the scattered radiation and the resolution time of the detector. The presented data give an opportunity to approximate the value of

both factors. The resolution time τ is a constant, whereas B depends on the value of $\mu\rho x$. B can be given by the general expression:

$$B = 1 + f\ (\mu\rho x) \tag{2}$$

Rewriting eq. 1 gives the following expression:

$$\frac{I_o B}{4\pi} = \frac{x^2 e^{\mu x}}{\frac{1}{I} - \tau} \tag{3}$$

In this expression the count rate I, the distance x, the theoretical value of μ and the mass density ρ expressed in equivalent units of water are known. Assuming various values of τ, one plot curves of the calculated $\frac{I_o}{4\pi} B$ values versus $\mu\rho x$. The two types of experiments performed, the first one with constant distance x (40 cm) and various values of ρ and the second one with constant ρ (water) and various distances x will give two deviating curves as long as the assumed value of τ is not correct. Eq. 3 shows that the calculated values of $\frac{I_o}{4\pi} B$ are much more sensitive to a variation in the distance x than to a variation in ρ. Practically it means that a same value of $\mu\rho x$ gives very different values of I in both experiments. The calculated values of $\frac{I_o B}{4\pi}$ at a short distance in water are much more sensitive for a variation in τ than the values calculated for a lower density at a distance of 40 cm to obtain a same value of $\mu\rho x$. Practically it means that the values of $\frac{I_o B}{4\pi}$ only coincide when the assumed value of τ is correct. The relation between $\frac{I_o B}{4\pi}$ and $\mu\rho x$ is presented in fig. 6 for the data of the experiments with the copper access tubes. The value of τ used is 120 μ sec. The curve drawn in this figure is given by the equation:

$$\frac{I_o}{4\pi} B = 8.2368\ 10^6 \{1 + 0.234\ (\mu\rho x) + 0.0812\ (\mu\rho x)^2 + 0.0157\ (\mu\rho x)^3 \tag{4}$$

A source of 20 mc, C_s^{137} gives approximately $7.4\ 10^8$ desintegration per sec, which results in a value of $\frac{I_o}{4\pi}$ of $5.8917\ 10^7$ counts per sec. Taking into account the effective area of the detector, it indicates that the efficiency of the detector is about 1%, which is normal for this type of detectors.

3.3. Deviation in distance

The most important requirement to obtain accurate data of wet bulk density and variation in moisture content is the parallelism of the two access tubes.

Though the construction of the equipment is such, that no large deviations can be present, as the positioning rods must be moved freely in the access tubes, small deviations may be still present when placing large tubes in the field. The results obtained in the preceding sections allow to calculate the effect of a deviating distance in terms of systematic errors in wet bulk density and change in water content. Fig. 7 presents the calculated curves valid for three values of x. The effect of 2 cm deviation in distance gives a systematic error in the derived wet bulk density of +7.2% when the spacing is too wide and -7.4% when the spacing is too small. The relation between the systematic error and the deviation from the distance of 40 cm is presented in fig. 8. The relation holds for values of $0.9\rho_s + \rho_w$ from 1.5 to 2.0. When the values of $0.9\rho_s + \rho_w$ become smaller than the systematic error slightly increases. As the error is systematically in one direction, the effect of a wrong distance on the change in water content is much smaller. In table 2 a comparison is given of the values of $0.9\rho_s + \rho_w$ measured by the γ transmission method and the data obtained by soil sampling between the two access tubes in a heavy clay soil and in a light sandy clay. The sampling was performed under extremely wet conditions at the end of a long term field experiment. The deviation in percent of the results of the gamma measurements are also given with respect to the mean value in each layer as obtained by sampling. Moreover, the corresponding deviation in distance is presented.

Table 2. Values of $0.9\rho_s + \rho_w$ as obtained by sampling and by the gamma transmission method in a heavy clay soil and in a light sandy clay

Depth cm	$0.9\rho_s + H_2O$ gr cm^{-3} sampling a	sampling b	sampling mean	gamma method	% deviation gamma method	error in distance Δx in cm
Heavy clay soil						
7- 12	1.462	1.739	1.596	1.552	-2.8	-0.82
17- 22	1.649	1.696	1.672	1.665	-0.4	-0.15
27- 32	1.626	1.632	1.629	1.670	+2.5	+0.58
37- 42	1.623	1.578	1.600	1.663	+3.9	+0.96
47- 52	1.655	1.648	1.652	1.696	+2.6	+0.61
57- 62	1.702	1.691	1.696	1.695	-0.1	-0.06
67- 72	1.660	1.673	1.666	1.713	+2.8	+0.66
77- 82	1.639	1.602	1.620	1.622	+0.1	+0.02
87- 92	1.717	1.599	1.658	1.632	-1.6	-0.50
97-102	1.594	1.603	1.598	1.669	+4.4	+1.11
Light sandy clay						
7- 12	1.663	1.668	1.666	1.552	-6.8	-1.84
17- 22	1.678	1.661	1.670	1.665	-0.3	-0.12
27- 32	1.727	1.677	1.702	1.670	-1.9	-0.58
37- 42	-	1.650	1.650	1.663	+0.8	+0.17
47- 52	1.582	1.682	1.632	1.696	+3.9	+0.97
57- 62	-	1.677	1.677	1.695	+1.1	+0.24
67- 72	-	1.658	1.658	1.713	+3.3	+0.80
77- 82	-	1.569	1.569	1.622	+3.4	+0.83
87- 92	-	1.610	1.610	1.632	+1.4	+0.31

The data in this table show that the calculated error in distance is not very large, as a part of the deviation will be caused by errors in the value of $0.9\rho_s + \rho_w$ obtained by sampling. The error due to non-parallelism of the access tubes will increase with depth. In the data given for light sandy clay a systematic deviation with depth seems to be present, but the calculations are based on a single sample at the greater depths, while the replications of the top layers show rather large differences. The same holds for the heavy clay soil. The large scatter in the data at 90 cm depth is mainly due to the boundary of the top clay layer with the underlying light sandy clay. However, the data do show that the parallelism of the access tubes can be reached under field conditions and that the deviations in the geometry are less than 1 cm.

4. Summary

A discussion is given of the use of the gamma transmission method for the measurement of soil moisture variations. It is shown that when using $0.9\,\rho_s + \rho_w + 1.01\,\rho_o$ as density scale a single calibration curve can be used for very different soils.

An approach is presented for the determination of the build-up factor of scattered radiation and for the instrumental resolution time.

It appeared to be possible to calculate the systematic errors due to non-parallelism of the access tubes in the derived value of $0.9\,\rho_s + \rho_w + 1.01\,\rho_o$.

5. References

DAVIDSON, J. M., J. W. BIGGAR and D. R. NIELSEN. 1963. Gamma radiation attenuation for measuring bulk density and transient water flow in porous materials. J. Geoph. Res. 68: 4777-4783.

GURR, C. G. 1962. Use of gamma rays in measuring water content and permeability in unsaturated column of soil. Soil Sci. 94: 224-229.

REGINATO, R. J. and C. H. M. VAN BAVEL. 1964. Soil water measurement with gamma attenuation. Soil Sci. Soc. Am. Proc. 28: 721-724.

Caption to figures

Fig. 1. Scheme of the exposure of the equipment under field conditions. 1 source; 2 detector; 3 connection frame of detector and source; 4 container; 5 counter; 6 access tubes for source; 7 access tube for detector.

Fig. 2. Calibration curves of count rate and density using various access tubes. . plastic tubes; o iron tubes; Δ copper tubes.

Fig. 3. Calibration curves of count rate and density using iron access tubes. 1 dry bulk density; 2 wet bulk density. The dashed lines connect points of equal dry bulk density in the dry and the wet experiment.

Fig. 4. The relation between count rate I times square of distance x and the distance between source and detector.

Fig. 5. The relation between count rate and the equivalent water density scale. o dry experiment $(0.9\,\rho_d)$; . wet experiment $(0.9\,\rho_d + \rho_w)$.

Fig. 6. The relation between $\frac{I_o}{4\pi} B$ and $\mu\rho x$; ρ is expressed in the equivalent water density scale.

Fig. 7. The calculated calibration curves of count rate and equivalent water density for 3 different distances (x) between source and detector.

Fig. 8. The calculated systematic errors in the equivalent water density and the error in distance (Δx) when using the calibration curve for x = 40 cm. The curve is valid for equivalent densities from 1.5 to 2.0 gr cm^{-3}.

C [illegible]

1. [illegible]

[illegible] for
direction.

[illegible] Cavity section [illegible] cavity using various waveguide tubes.

[illegible] plane-to-tube [illegible] tubes.

Fig. [illegible] Cavity for [illegible] low-frequency tests.

[illegible] built-[illegible] [illegible] to d[illegible] [illegible] three coaxial cavity
[illegible] [illegible] [illegible] [illegible] current.

[illegible] The [illegible] [illegible] [illegible] and the
dielectric [illegible] [illegible].

Fig. 7. [illegible] [illegible] [illegible]

fig.1

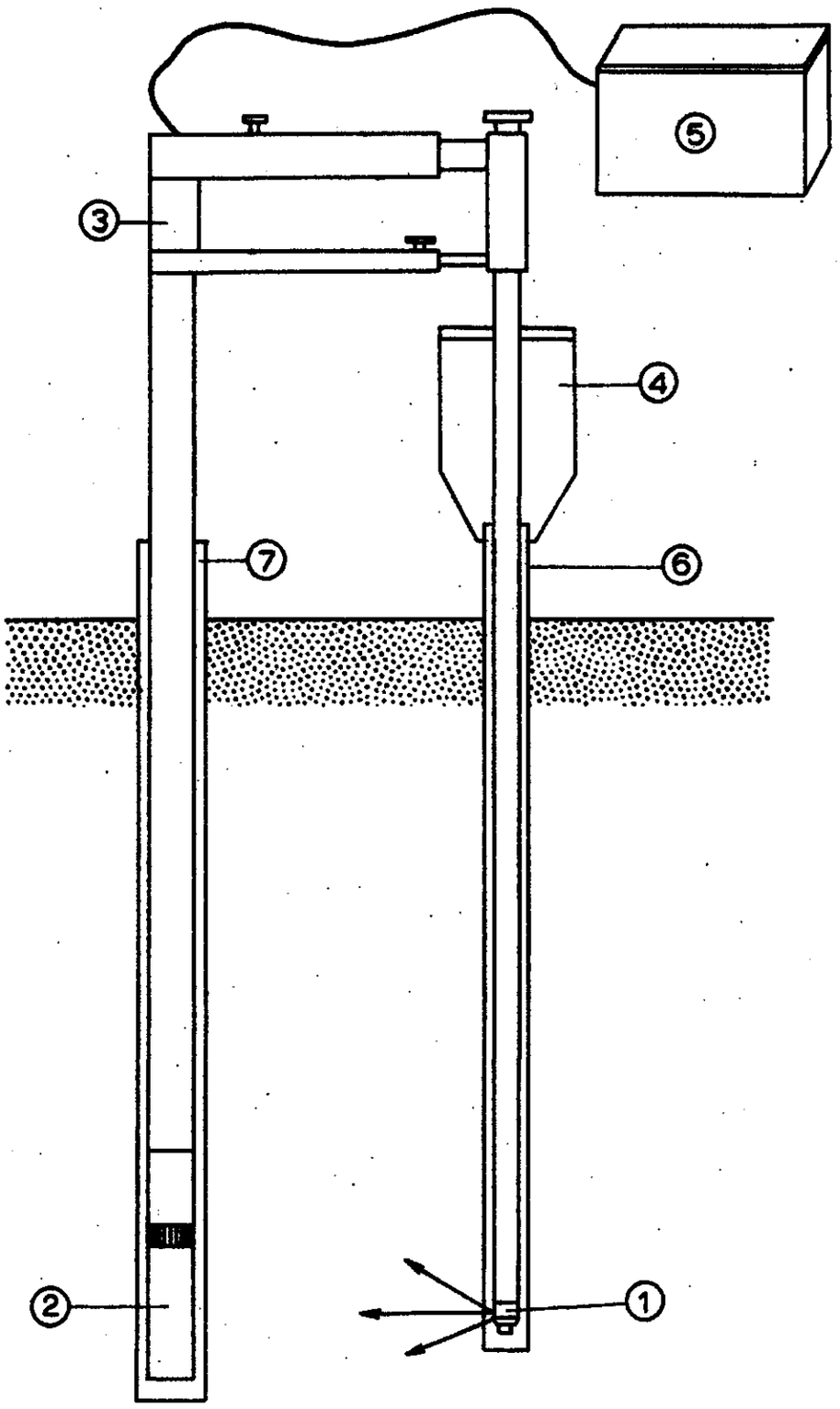

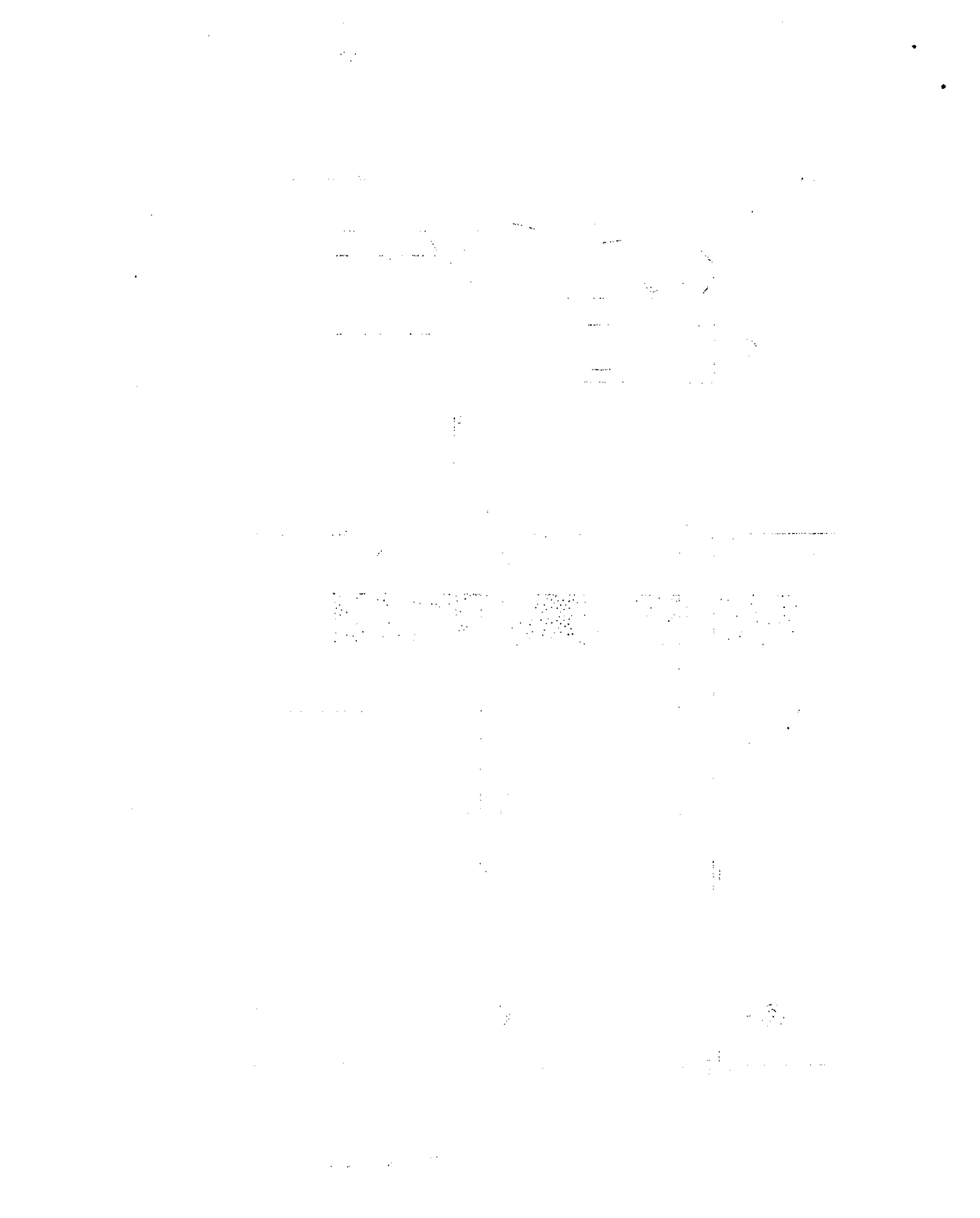

fig. 2

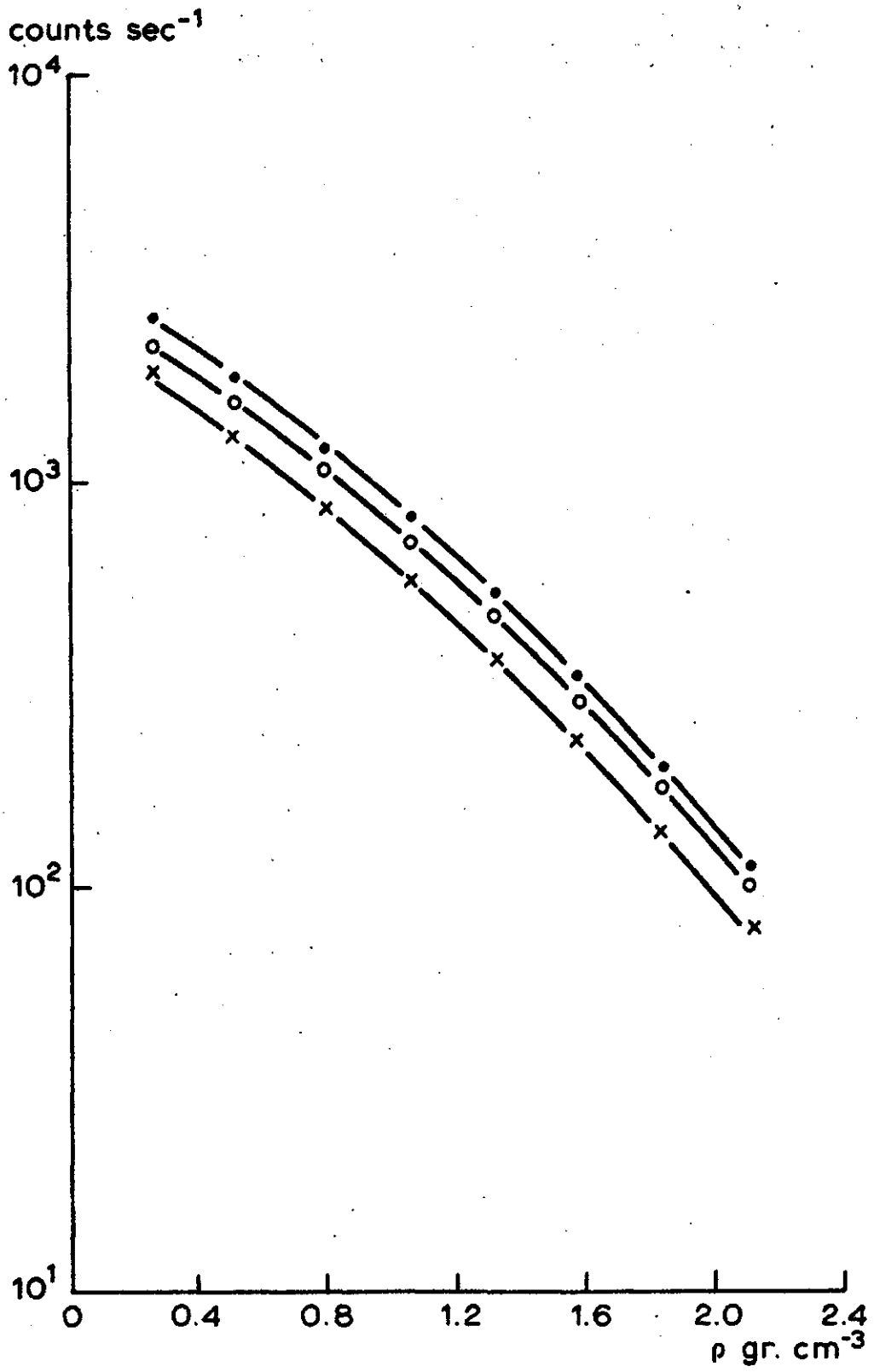

68C.82.2/2.9

fig. 3

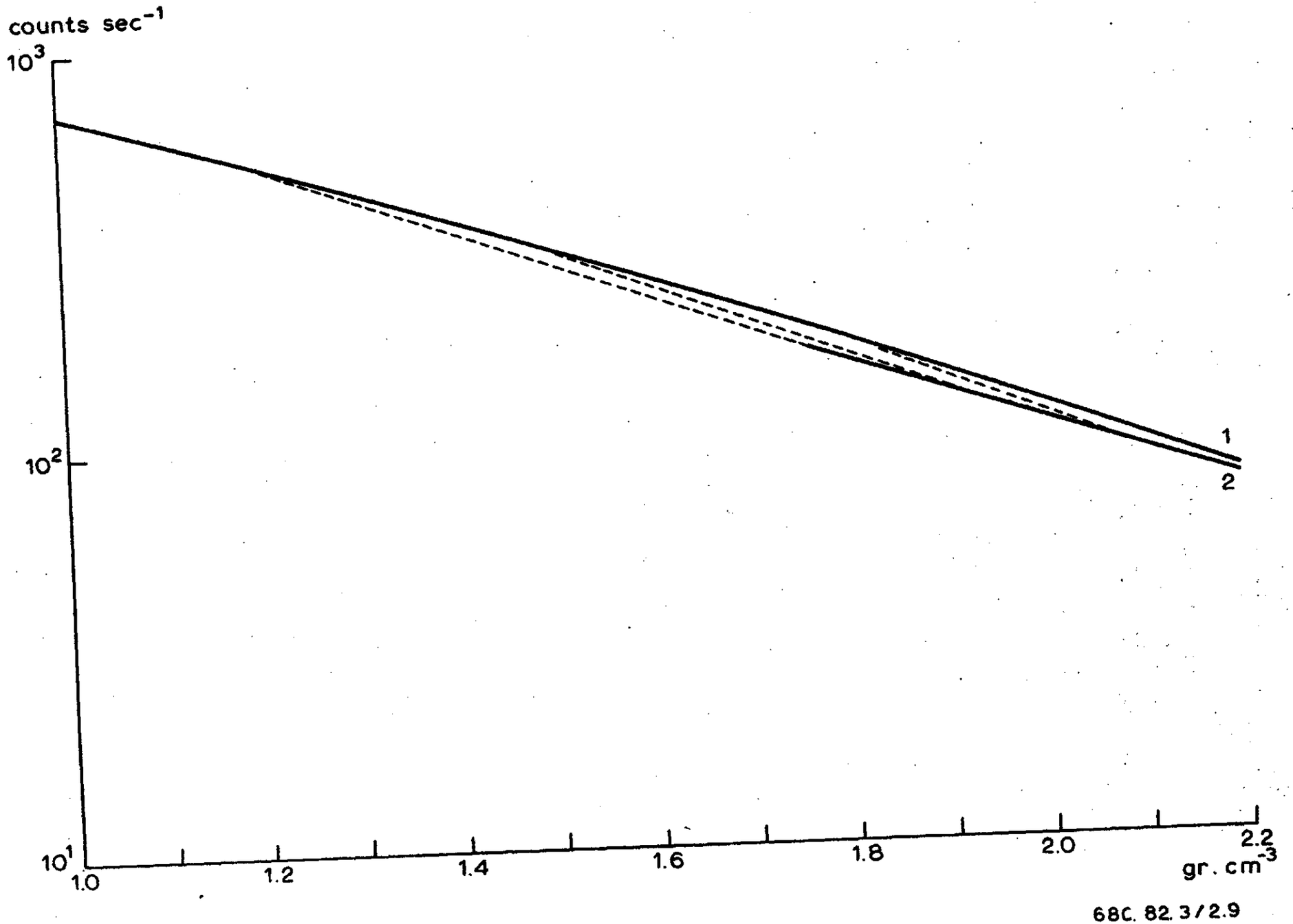

68C. 82.3/2.9

fig. 4

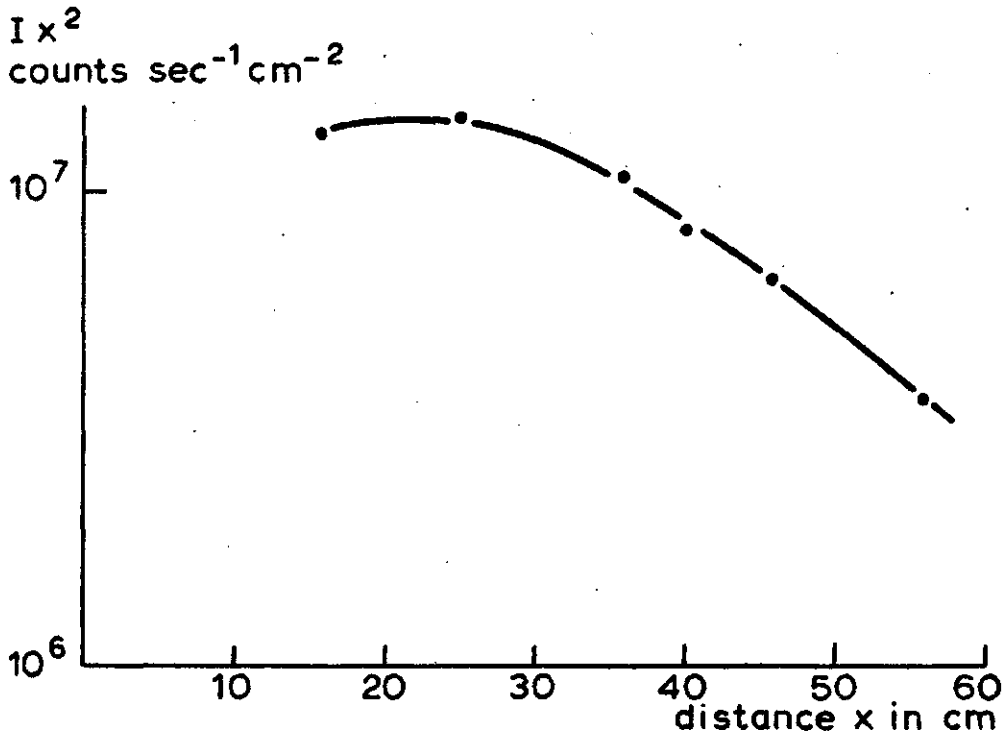

68C. 82.4/2.9

fig. 5

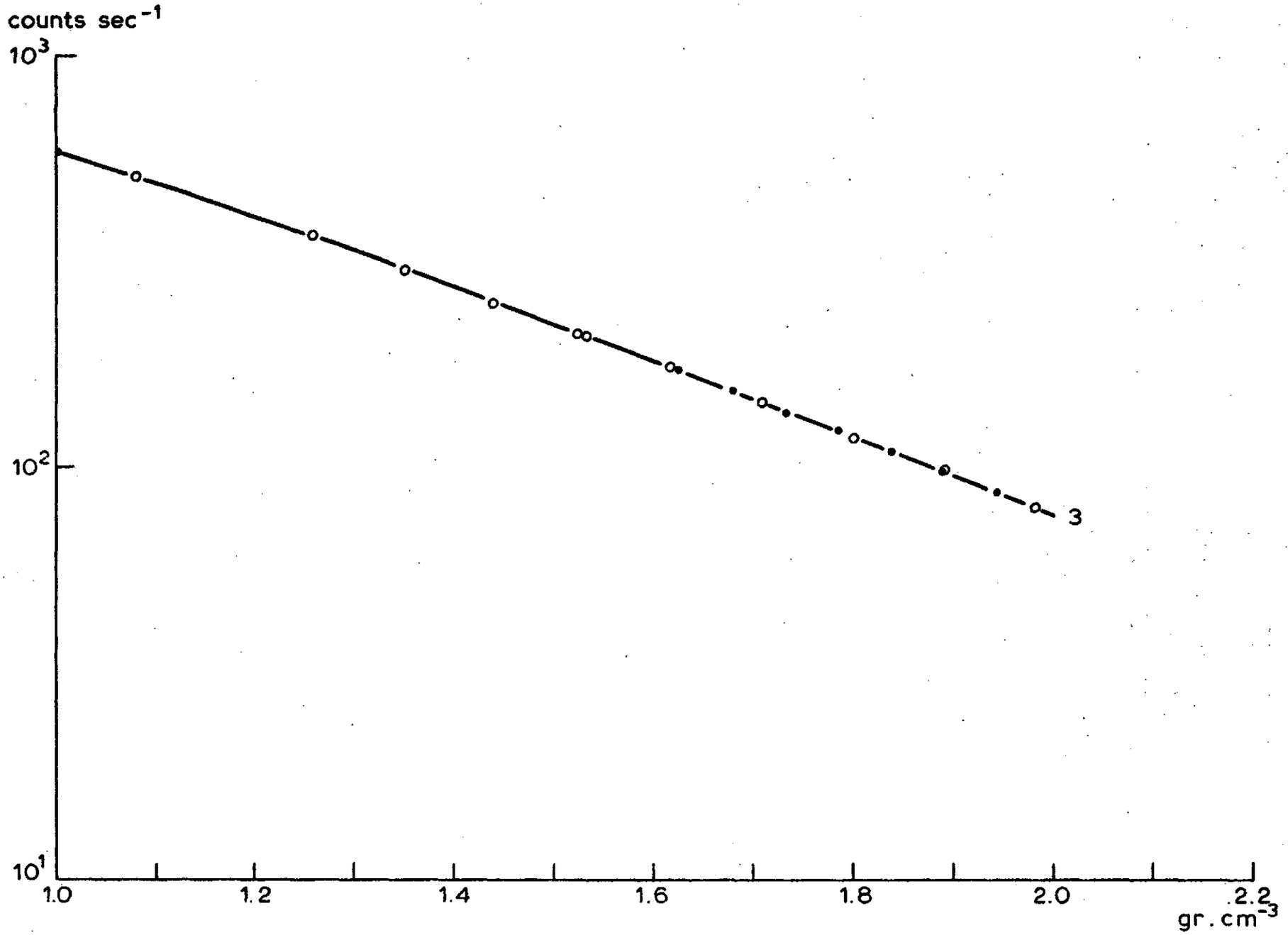

68C.82.5/2.9

fig. 6

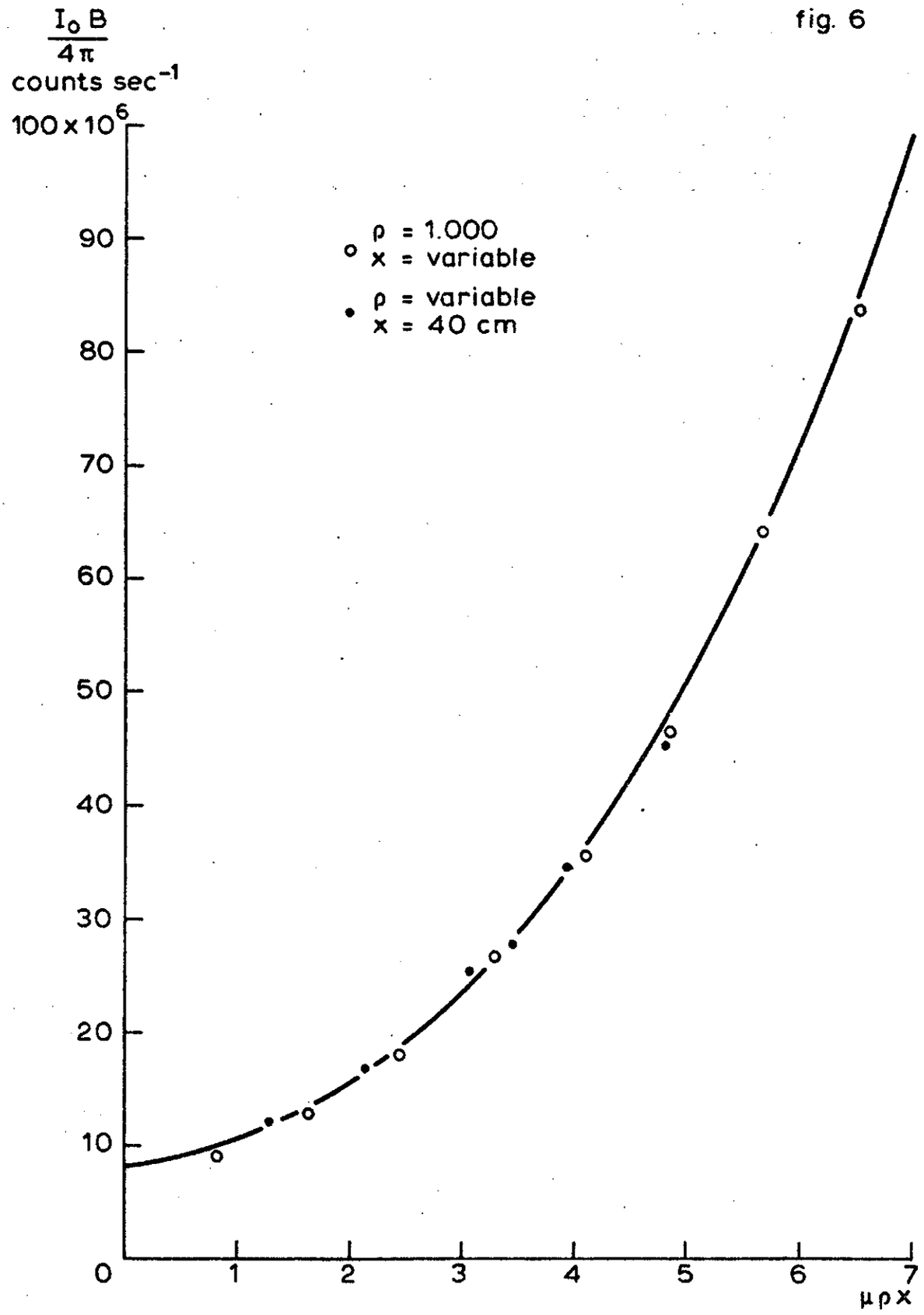

68C.82.6/2.9

fig. 7

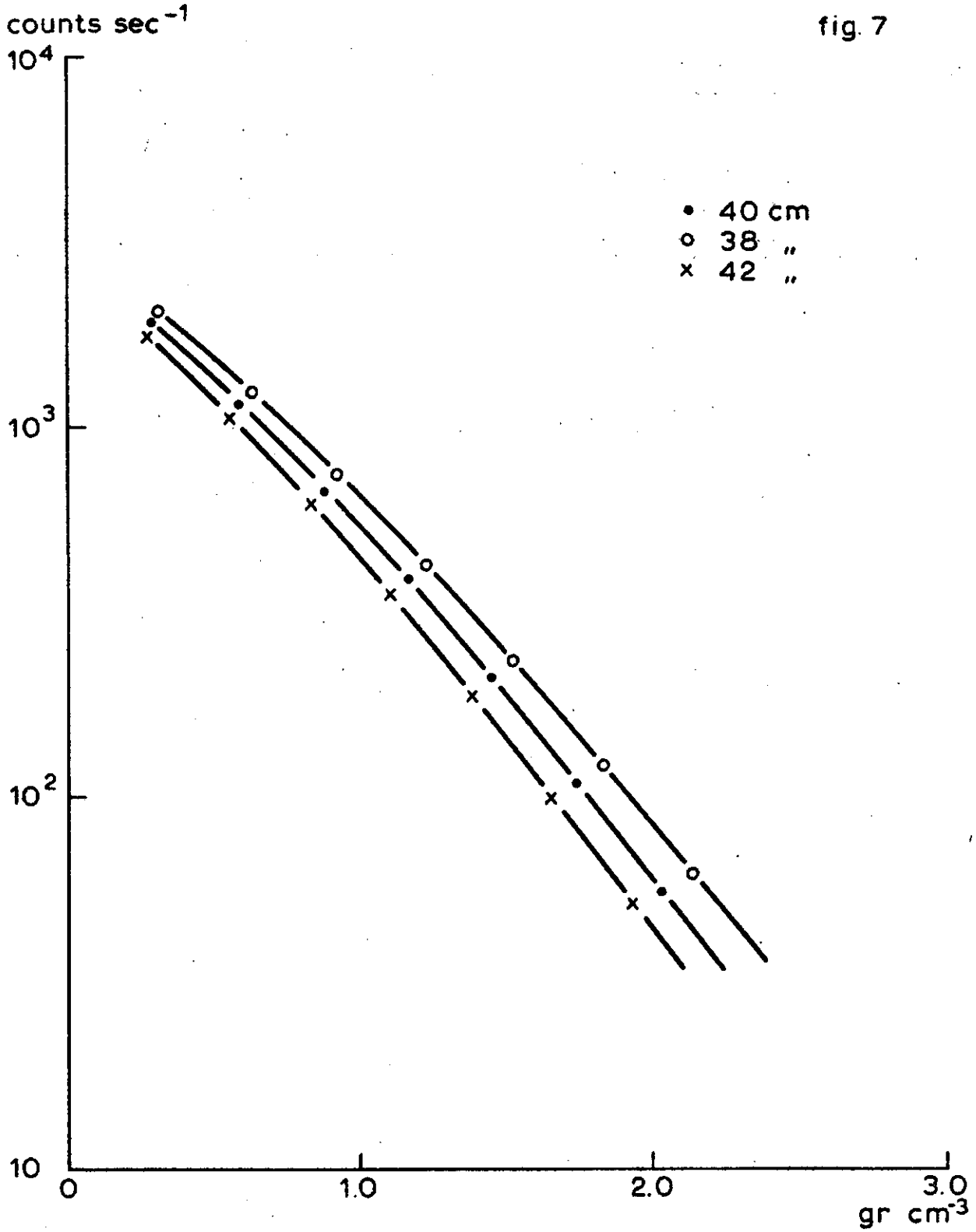

68C.82.7/2.9
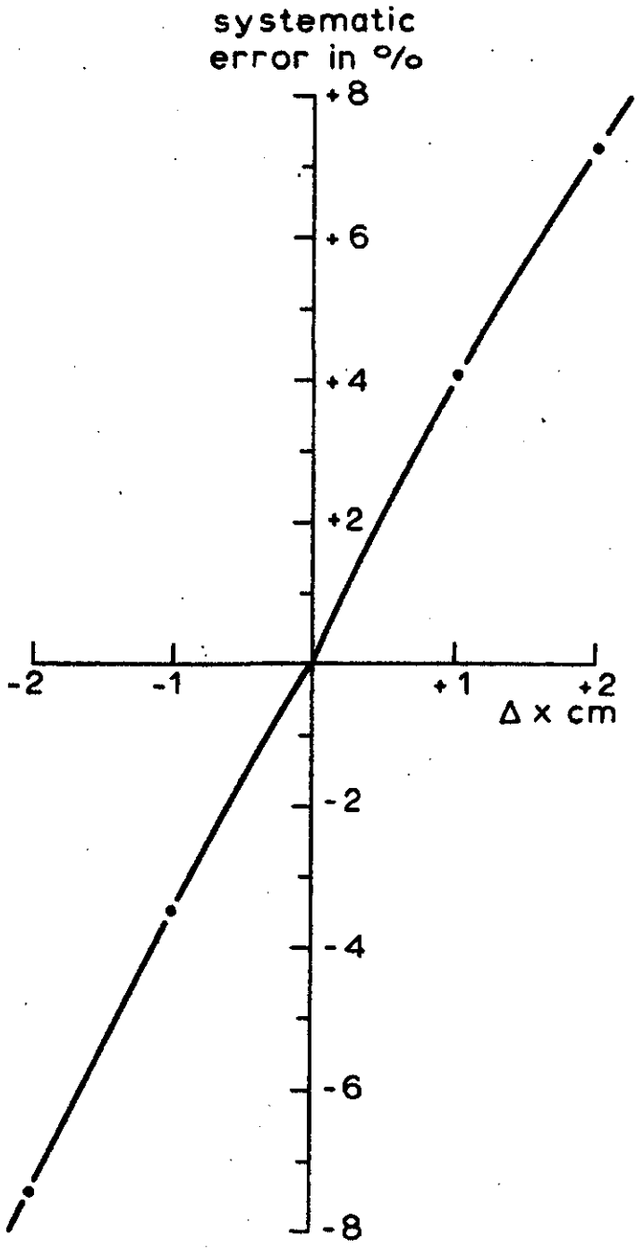
fig. 8